International Journal of Thermofluids 24 (2024) 100944

Contents lists available at ScienceDirect

International Journal of Thermofluids

journal homepage: www.sciencedirect.com/journal/international-journal-of-thermofluids

Optimization of an innovative cooling system for motorsport application

Leone Martellucci *, Roberto Capata

Department of Astronautics, Electrical and Energy Engineering, Sapienza University of Rome, 00184, Rome, Italy

A R T I C L E I N F O

Keywords:
Air-cooling
PCM
Thermal management
Battery
Formula student

A B S T R A C T

One of the most critical issues in electric vehicle engineering concerns the thermal management of the battery pack, especially in high-performance applications, which are increasingly demanded by the market. Very interesting, from this point of view, is the study of motorsport applications, almost always characterized by a high ratio between power output and energy stored in the battery pack, which makes the problem of thermal management particularly important. It should be noted that motorsports applications typically have a particularly demanding trend of current discharging and charging from the battery pack, with numerous positive and negative peaks at high c-rates; this obviously produces, due to the Joule effect, a much higher amount of heat per kWh than in conventional road cars and therefore makes efficient and high-performance thermal management very important. In this work was defined, analyzed and optimized an innovative mixed solution with forced air cooling and PCM material (phase change material) for high performance battery modules with cylindrical cells used in a Formula Student car. In the various battery thermal management technologies, Air cooling is one of the most used solutions and can be successfully integrated with PCM cooling technique. In the work proposed here, the optimization and numerical simulation of different solutions and configurations is described. The target parameters considered are: airflow rate, cell spacing and mass of PCM. Fluid dynamic simulations were used to identify the optimal value of the radial gap between the cells, a fundamental construction parameter, and the speed of the air coming out of the fans. The choice of the mass of the PCM sheets was made on the basis of the quantity of heat to be removed to obtain a significant effect on the final temperature of the cells during the test ($<50^{\circ}C$) and compatibly with the spaces available between the modules inside the battery pack. The simulations of the optimal solution will be compared to experimental results for validation, by the realization of the most promising configuration and its real experimentation on the car, in order to validate the expected performance of the thermal management system.

1. Introduction

Li-ion batteries produce heat during the charge and discharge operations and the temperature of the cells must be strictly maintained within optimum working temperature range 20-40°C in order to keep the internal resistance of the individual cells low and thus ensure maximum performance. Thermal issues like overheating and uneven temperature distribution can lead to rapid cell degradation and shorten battery life. In extreme cases, thermal runaway may also occur when the cell temperature rises above the limit, in which this high temperature triggers the exothermic re-actions in the operating cells. These reactions release more heat led to an uncontrolled heat generation causes fire or explosion. Thus considering, one of the major concerns in the development of lithium-ion battery packs is thermal management. Similar to conventional ICE vehicles, a battery pack in EVs and HEVs need a cooling system. Different types of cooling system technologies will influence the performance and cost of the battery pack thermal management system. Over the last two decades, many batteries thermal management technologies have been developed to maintain the optimum temperature range in the battery packs namely,

1) The Air-cooling method classifies into Natural & Forced Convection
2) The Liquid-cooling method classifies into Indirect & Direct cooling
3) Thermal storage method such as Phase Change Material
4) The Heating method classifies into Self-internal heating, Convective heating, and Mutual Pulse heating.

Compared with the above technologies, the air and liquid cooling are most widely used methods to fulfil the requirements of automotive industries, but Phase Change Materials are a very promising technology

* Corresponding author.
E-mail addresses: leone.martellucci@uniroma1.it (L. Martellucci), roberto.capata@uniroma1.it (R. Capata).

https://doi.org/10.1016/j.ijft.2024.100944

Available online 14 November 2024

especially in terms of simplicity and low cost. This work intended to focus on a mixed forced air-cooling and PCM cooling with a simple design, low manufacturing cost, light, easy to maintain and with a high overall reliability.

In the Air-cooling battery thermal management solution, the air is the cooling medium and removes the heat generated by the battery cell. This cooling method is classified into Passive cooling (Natural convection) and Active cooling (Forced Convection) [1–3]. The former passive (only ambient environment used) typically used for low-density batteries, and the latter active (special components provide for heating or cooling at cold or hot temperatures) use fans/blowers to enhance convection [4,5]. PCM cooling, used in conjunction with forced-air cooling, adds a kind of thermal booster to the system above the liquefaction temperature of the PCM, which must be chosen consistently with respect to the temperature window of the lithium cells.

2. Battery pack description

We would like to describe here the process of designing and defining the forced-air thermal management system applied to a Formula Student single-seater car, characterized by a high ratio between maximum power output (80 kW) and stored energy (8 kWh).The Formula Student electric car is equipped with a storage system placed is in the central part of the chassis, in backside position respect of the driver seat. The cockpit of the single-seater car and the battery pack are separated by a fire-retardant wall made in aluminum and Kevlar, which guarantees electrical insulation and segregation of flames in the event of breakdowns. The battery pack is made up by six modules connected in series, in an electrical configuration with string of 108 parallels of 7 cells, 108s7p configuration. Each module is a 18s7p assembly, with 75.6 V of maximum voltage and 1.58 kWh of maximum stored energy. In Table 1 the whole battery pack specifications are reported and in Fig. 1 and Fig. 2 the cell specifications and performance graphs are reported. In Fig. 3 and Fig. 4 CAD drawing and photo of the battery pack are presented.

3. Methodology and CFD analysis: the battery module

The methodological basis used to arrive at the optimal configuration of the mixed cooling system with force air and PCM material is described in this section.

First, the geometric configuration of the cells was analyzed, which together with the force air flow produced by the fans, optimizes the forced-air cooling alone. Thus, the target variables to be optimized are the spacing between the cells and the air flow rate produced by the fans, which are equipped with PWM-type speed control. Subsequently, considering only the optimal configuration with forced-air cooling, the optimal amount of PCM material to be used was studied to further improve the performance of the cooling system. Therefore, the design and optimization was developed in two successive phases, the first leading to the definition and realization of the battery pack with only forced-air cooling for the 2022 season of Formula Student Championship, and the second, for the 2023 season, involving the use of special plastic bags with PCM material inside to be placed on the module busbars, compatible with the geometries of the 2022 station battery pack.

Table 1
Battery Pack Specifications.

Cell type	Cylindrical
Cell manufacturer	Sony
Cell model	US18650VTC6
Electrical Configuration	7p108s
Nominal Voltage (V)	388
Maximum Voltage (V)	450
Total Energy (kWh)	8.1
Container Dimensions (mm)	494 × 463 × 238
Container material	Kevlar fiber
Total Weight	54 kg

Initially, a CFD analysis on the air-cooling battery thermal management solution method has been studied using ANSYS FLUENT software. The battery module has 126 Cylindrical Li-ion cells of 18650 format, arranged electrically in 18s7p configuration and geometrically positioned linearly in 9 rows of 14 each (see Fig. 5).

The thermal properties of single cell are reported in Table 2, where the most important parameters used for CFD thermal model are axial and radial thermal conductivities.

The forced air-cooling path in the battery module involves two inlets and two outlets ports (see Fig. 5). When the air enters from the two inlet ports, the air flow is used to cool down the batteries arranged in series and the air temperature rises due to its low heat capacity and this leads to higher cell temperatures at the module outlet ports. two identical split paths have been provided precisely to reduce the temperature delta between air inlet and outlet in the module. Moreover, some significant measures were taken to improve the cooling performance in the module by increasing the cooling speed, optimizing the position of each cell arranged side by side in a rectangular pattern, and positioning fan on top of the battery module. Another important factor taken into consideration is the split airflow, which can significantly improve the thermal performance of the battery module. The configuration has both inlet and outlet ports in the top of the module, where it can create the flow moving forward and backward.

Battery cooling is directly proportional to the heat generated inside the battery. The most common equation describing heat generation in a battery cell during an electrochemical process (charge or discharge) is given by:

$$q = I\cdot(V_O - V) - I\cdot T\left(\frac{dV_O}{dT}\right) \tag{1}$$

where q is the heat generation in the battery cell, V_0 is the open-circuit voltage, V is the cell voltage, I is the applied current and T is the temperature of the cell.

From the equation (1), the first term of the equation represents the overpotential due to the ohmic losses and charge transfer at the interface. The second term represents the reversible entropic heat from the reaction [6,7].

When a current flow in a battery, the cell voltage V deviates from the open-circuit voltage V_0 because of electrochemical polarization. The resulting energy loss is converted into heat. This heat can be calculated using the internal resistance and current of the cell. The cells are assumed as a constant heat source.

This heat generation can be expressed as overpotential heat Q:

$$Q = I\cdot(V_O - V) = I^2\cdot R \tag{2}$$

Q represents heat generation during both charging and discharging. Expressing the difference between V and V_0 by I•R. R is the overpotential resistance related to Q [8,9].

If the heat generation rate per unit time and volume, the equation (2) represents:

$$Q = I^2R/Vol \tag{3}$$

where Vol is the effective calculating volume of the battery module. In Table 3 the single cell heat generation data are collected.

The values of the radial distance between cells were chosen according to the most relevant boundary conditions. The minimum value, 1.5 mm, was chosen to minimize the risk of electrical shorting during assembly; in fact, it should be considered that the cells are “naked,” i.e., without the plastic wrap normally used, so as to improve heat exchange with the air, but of course, as noted, the naked cell has the outer shell in conduction with the negative pole. Also, for making the holders that hold the cells, going below 1.5 mm makes the machining more

Model	Sony US18650VTC6	
Nominal Capacity	3120mAh	
Nominal Voltage	3.6V	
Weight (Approx.)	46.4 ± 1.5g	
Initial Impedance	12 mΩ	
Dimensions	Diameter	18mm
	Length	65mm
Nominal Charge Condition	Current	3120mAh (1C)
	Voltage	4.2V
	Cut-off current	62mA (0.02C)
	Ending time	2.5h
Nominal Discharge Condition	Current	3120mAh (1C)
	Cut-off Voltage	2.0V
Continuous Maximum discharge current	15A/30A (5C/10C)	
Temperature Condition	Charge	0°C to 45°C
	Discharge	-20°C to 60°C
	Storage	-5°C to 35°C

(a)

(b)

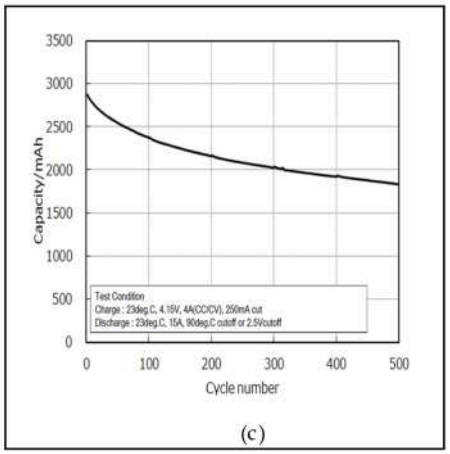

(c)

Fig. 1. Sony US18650VTC6: (a) Cell Properties, (b) Cell Model, (c) Cycle Life.

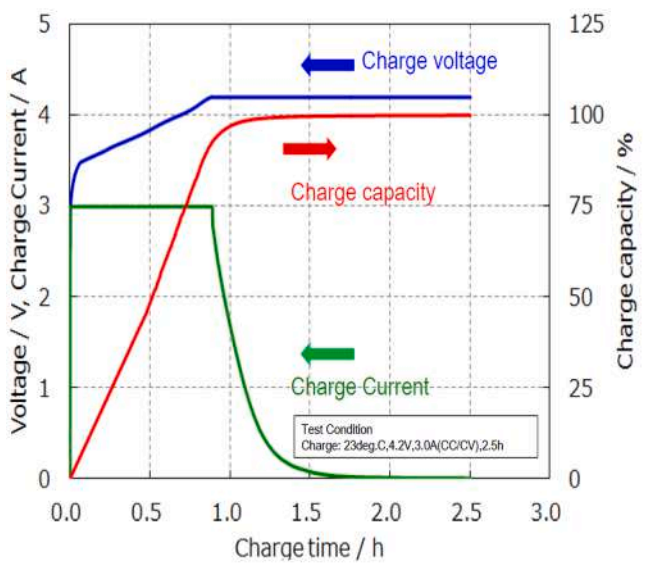

(a)

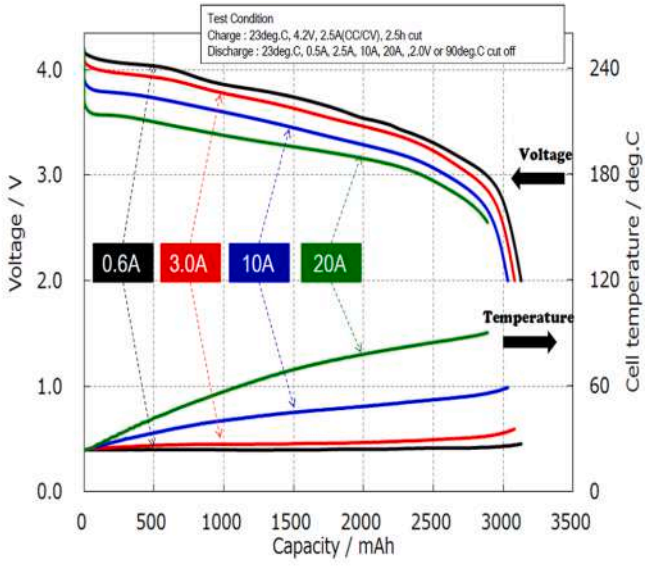

(b)

Fig. 2. (a) Charge Characteristics, (b) Discharge Characteristics.

expensive and the holder itself less durable. The maximum value, 2.5 mm, was chosen compatibly with the space available for the individual modules and the volumetric energy density required by the battery pack design.

C-Rate is a relative measure performance of the battery [10]. Charge and discharge rates are governed by C-rates. For instance, a 1C discharge rate would deliver the battery rated capacity in 1hr, and 2 C discharge rate means it will discharge twice as fast in 30 minutes. In this work, 1.5 C-rate and 3 C-rate were taken into consideration for simulations.

The forced-air cooling technic, that rely on an external device (cooling fan) to enhance the heat transfer, allows to use cooling fans to cool down the battery and to maintain the optimum temperature range

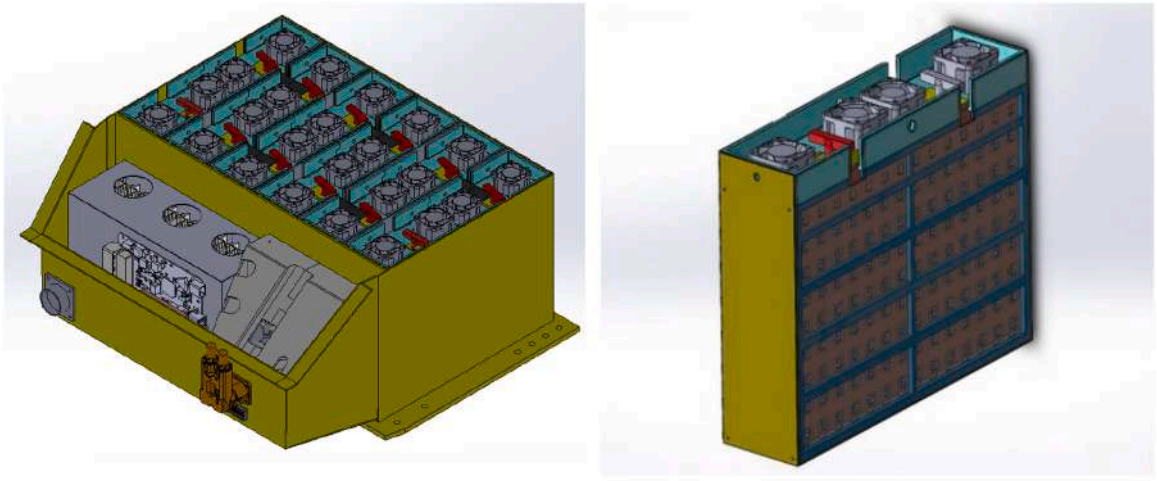

(a) (b)

Fig. 3. (a) Assembly of Battery Pack, (b) Assembly of Battery Module.

Fig. 4. Battery Pack installed on the vehicle.

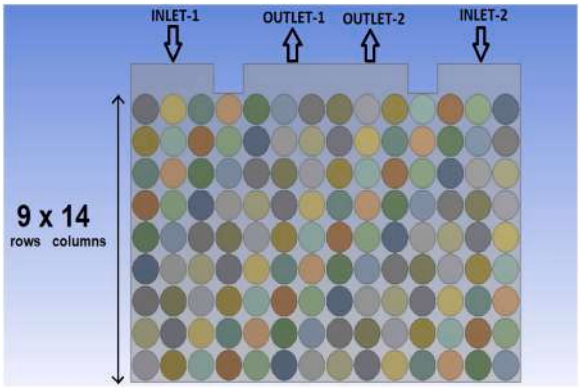

Fig. 5. Battery module geometry.

for the battery, with the additional function of the rate of fluid flow modulation through fan speed control to increases the heat removal rate. Adding a properly sized cooling fan to this battery module will force air across the module and allow the greater thermal transfer. In Table 4 the cooling fan specifications are collected.

Table 2
Sony VTC6 thermal properties.

Rated Discharge Capacity (1C-Rate)	3.12 Ah
Nominal Voltage	3.6 V
Rated Discharge Energy	11.1 Wh
Density	2800 kg/m^3
Heat Capacity	950 J / (kg•K)
Radial thermal conductivity	1 W/ (m•K)
Axial thermal conductivity	25 W/ (m•K)

Table 3
Heat generation of the cell.

Distance between the cells	Discharge rate	Current of the cell (A)	Heat generation per cell (W)	Heat generation rate (W/m^3)
1.5mm	1.5 C	4.68	0.3	11000
	3 C	9.36	1.2	43700
2mm	1.5 C	4.68	0.3	10415
	3 C	9.36	1.2	41652
2.5mm	1.5 C	4.68	0.3	9921
	3 C	9.36	1.2	39685

With these information it is possible to study the optimal cell spacing and air flow speed for the better cooling condition; all the simulations are performed under constant current discharge conditions, as the goal has been to compare the overall performance of the air-cooling method for different flowrates mentioned as 3 m/s to 6 m/s for 1.5 C-rate of discharge and 6 m/s to 11 m/s for 3 C-rate of discharge.

All fluid-dynamic simulations performed assume an ambient air temperature of 25°C, which thus represents the temperature of the air entering the module downstream of the fans. Fluid dynamic simulations were performed using the Multi-scale and Multi-dimensional (MSMD)

Table 4
Cooling fan specifications, 4 fans for each module.

	0.3W/Cell (Equivalent to 1.5C)	1.2W/Cell (Equivalent to 3C)
Coolant type	Air	Air
Dimensions	60 • 60 • 38 mm	60 • 60 • 38 mm
Air velocity	3 to 6 m/s	6 to 11 m/s
Air flow	40 to 82 m^3/h	82 to 142 m^3/h
Rated Voltage	24 V	24 V

battery model and conjugate heat transfer approach in Ansys Fluent. The geometric model of the module was reproduced in 3D, see Fig. 6, with the areas where the installation of the cooling fans is planned highlighted (the four parallelepipeds in Fig. 6 on the upper face of the module); the boundary conditions include the presence of the air speed produced by the fan in the inlet area corresponding to the dimensions of the impellers of the four fans installed on the upper face of the module, while the manometric pressure is maintained at atmospheric pressure at the output surfaces. The inlet flow is considered turbulent, and inlet velocities will be between 3 m/s and 11 m/s, depending on the performance of the chosen fans. The simulations converge rapidly, after about 80 iterations, see Fig. 7.

As for the mesh independence analysis, three different meshes were considered, with a polyhedral grid and with a characteristic cell size of 0.5 mm, 0.2 mm and 0.1 mm, respectively. The control volume and the calculation field correspond to the left portion of the module, relying on the perfect symmetry of the module, in order to reduce the calculation time. The total number of cells in the structured mesh, for the considered volume, corresponding to the size of 0.5 mm is equal to 2.08 million, and grows proportionally for the 0.2 mm and 0.1 mm meshes to 8.1 million and 32.4 million, respectively. Fig. 8 shows the mesh independence analysis, using as a reference quantity the average temperature at the outlet in the case with a radial gap between the cells of 1.5 mm (the smallest among those chosen), discharge at 3 C-rate and fan speed at 11 m/s.

In order to estimate the impact of cells spacing gap (1.5 mm, 2 mm and 2.5 mm) and the air-flow speed supplied by fan system, the various configurations have been analyzed for 1.5 C-rate and 3 C-rate, corresponding to 0.3 W and 1.2 W of heat generation per single cell. In Fig. 9 the temperature maps of the module are reported, for 1.5 C-rate and a two air flow speeds; as expected, the hottest cells are in central position, but the difference between hottest and coldest cells (ΔT in the following) do not exceed 4°C, a good value for an auto-motive application. At higher flow speed, 6 m/s, the forced air cooling is able to perform an adequate cell cooling and a good temperatures distribution along the module. In Fig. 10 the same module geometric configuration (1.5 mm of air gap between cells) is simulated at a discharge current equal to 3 C-rate, for a new set of fan flow rates, starting from 6 m/s (in order to compare the results with 1.5 C-rate case) to 11 m/s.

In this case, the ΔT rise noticeably and reaches the value of 12°C for the case with an air flow speed of 6 m/s; with an air flow speed of 11 m/s the ΔT decrease to a value of 6°C, an optimal value for automotive applications. The 3 C-rate is equivalent to 28 kW of power supplied by the whole battery pack to the electric drive, that is power output similar to the average power utilized during "Endurance" Formula Student event. Thus, this case represents an interesting thermal test of the cooling system.

Analyzing the influence of the space between the cells on cell temperatures with forced air cooling under various conditions, it is possible to observe that the increased air gap reduces the air speed in the streamline between cells and, as consequence, the heat removal is less efficient, without any advantage in air flow friction reduction. In Fig. 11 the temperature distribution with 1.5 mm of cell spacing, 11 m/s of air speed, 3 C-rate discharge and 1.2 W/Cell is compared with the same conditions but with 2 mm and 2.5 mm of cell spacing.

It is evident that the maximum temperature in the module is rapidly increasing as the gap increases between the cells, which means the thermal performance is deteriorated. It is found that the spacing significantly affects the temperature uniformity. From the increased air speeds with the three spacing sizes of modules, it is observed that the flowrate increases at the inlet and decreases near the outlet as the gap increases. Thus, the uneven temperature distribution of the air flowrate leads to a higher temperature difference in the case of 2mm and 2.5mm distance be-tween the cells. When the gap decreases, the uniformity of the air flowrate between the cells is improved, which can help to reduce the temperature difference of the battery pack and also to increase the convective heat transfer coefficient on the surface of the cells which reduce the cell temperatures.

As reported in Fig. 12, ΔT in the module is gradually increasing when the gap increases. This work suggests that the optimal spacing for the lowest maximum temperatures is the smaller air space 1.5 mm. And the smaller spacing would be preferred because of the packaging constraints of the battery systems in vehicle.

The comparison of all the simulations at 1.5 C-rate shows that the configuration of 1.5 mm spacing with the velocity of 6 m/s is giving the better result of maximum temperature is 23.7°C and the maximum

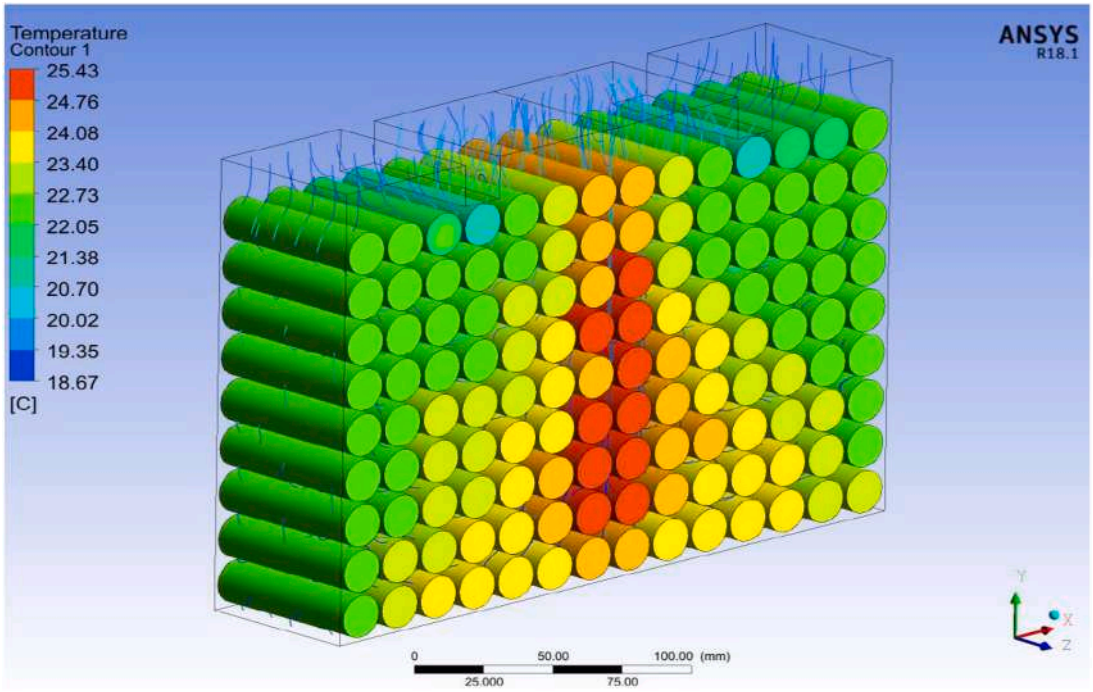

Fig. 6. The geometric model of the module in 3D.

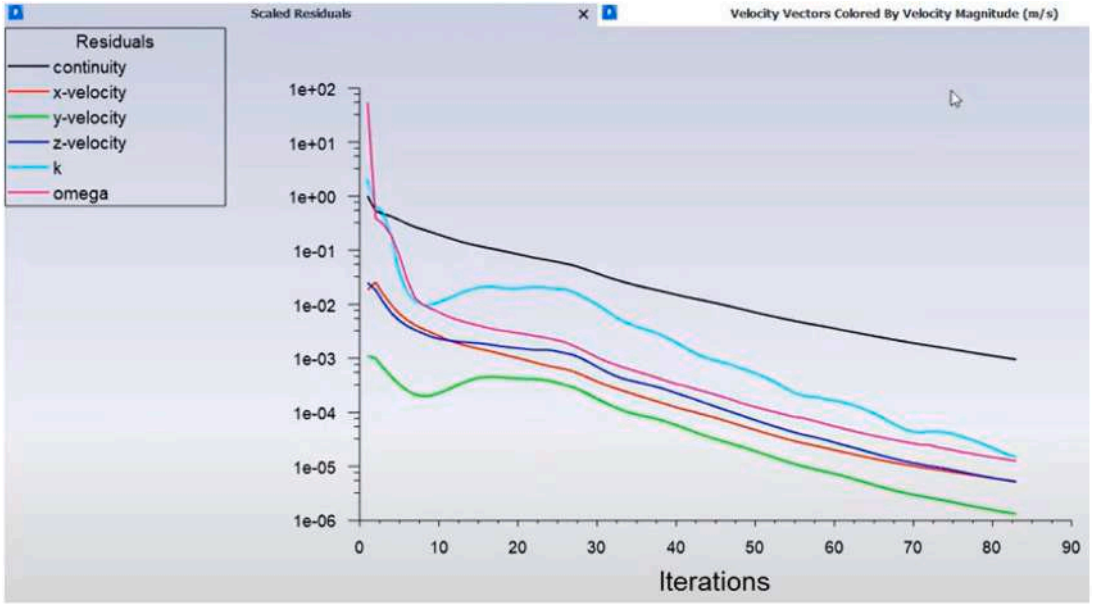

Fig. 7. Convergence of the calculation.

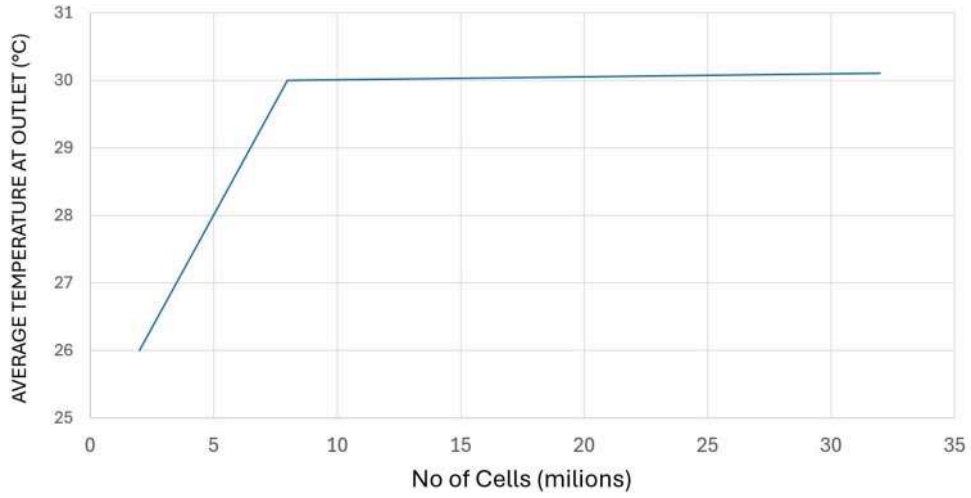

Fig. 8. Mesh independence study.

temperature difference in the module is 2.5°C. At 3 C- rate, the configuration of 1.5 mm spacing with the velocity of 11 m/s is giving the better result of maximum temperature is 32.4°C, and the maximum temperature difference in the module is 6.2°C.

4. Thermal performance of the battery pack

The results of the CFD simulations discussed in the previous paragraph defined the design and construction of the battery pack installed on the Formula Student car for the 2022 season. Therefore, the pack was equipped with a forced-air cooling system with 4 fans (Table 4) per module, for a total of 24 fans, and the modules with 18650 cells have a cell gap of 1.5 mm. The rotation speed of the fans is managed by the vehicle's VCU as a function of the average temperature of the battery pack so as to obtain an air inlet speed of between 0 m/s and 11 m/s into the modules. The car has participated in official Formula Student events in Italy (Formula SAE Italy 2022) and Spain (Formula Student Spain 2022). The cell temperature data acquisitions (minimum temperature and maximum temperature) were used to verify the CFD analysis of the battery pack cooling. Fig. 10 shows the temperature trend of the hottest cell during the Endurance test at the Italian event held at Varano de' Melagari. The temperature trend highlighted some criticalities that did not emerge in the CFD simulations. In fact, the temperature of the hottest cell reached almost 60°C with an increase of around 25°C compared to the initial temperature. In fact, therefore, it almost reached the permissible regulatory limit above which the car must be switched off and the pack disconnected. The reasons for this trend are undoubtedly the average power supplied by the individual cell, which is slightly higher than that hypothesised for the CFD (1.3 W against 1.2 W). The particularly high ambient temperature (35°C) and the management of the speed of the fans, which, in order to limit the electrical consumption of the fans themselves, only used the maximum rotation speed (corresponding to the 11 m/s speed of the air entering the modules) when the cells reached 45°C, also contributed negatively. This management logic made it possible to complete the Endurance test without exceeding 60°C, but penalised the performance of the powertrain due to the increased internal resistance of the pack between 50°C and 60°C.

Fig. 13 shows the initial cell temperature value (35°C) and the practically constant temperature during the pilot change phase (between 600 s and 800 s). The final value of cell temperature reach 60°C,

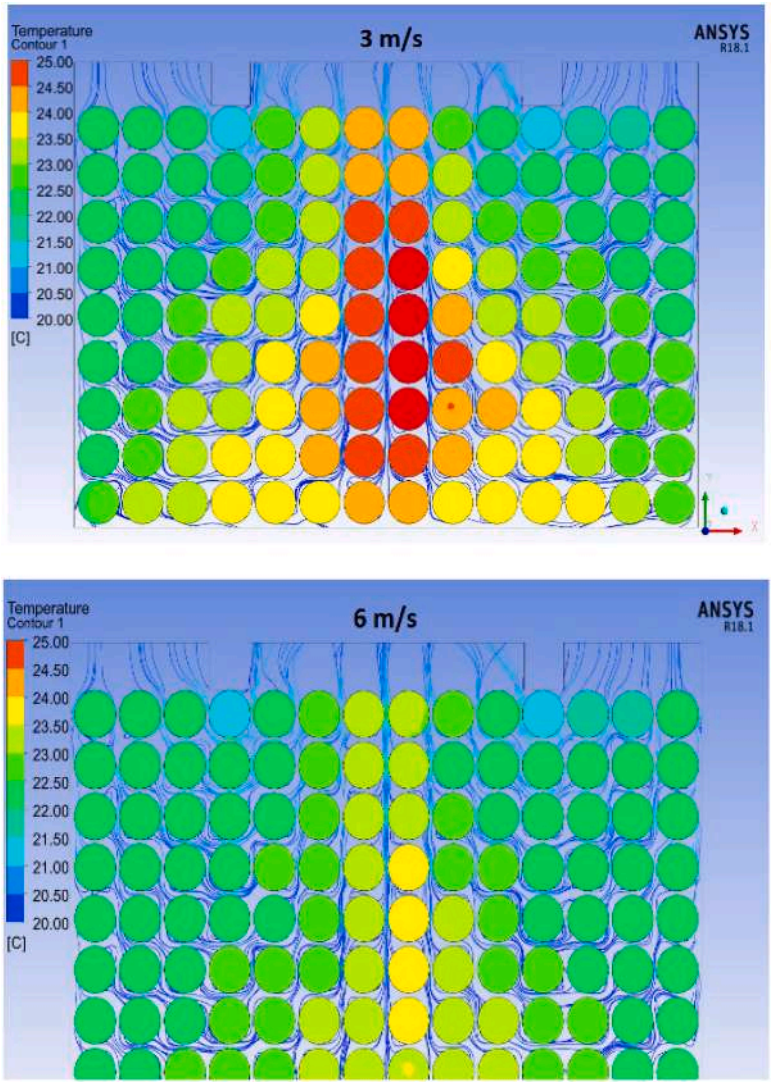

Fig. 9. Temperature distribution with air cooling at 3 m/s and 6 m/s in the 1.5 mm spacing configuration and 1.5 C-rate discharge, with 0.3 W/Cell of heat production.

the maximum limit admitted by the competition rules.

These experimental measurements suggested that the thermal management of the battery pack could be further improved for the 2023 season; the idea is to use a passive solution, which does not entail any energy consumption and involves a minimal increase in battery pack weight. It was therefore decided to design and then experiment with a solution using PCM (phase change material).

5. PCM pouch system, design and performance

The phase change materials have high latent heat and acts as a heat sink during battery discharge. When the cells are on standby, the PCM releases heat to the cells and the environment. The PCMs used for thermal management have a melting point in the optimum performing range of lithium cells. In can be used to help the cell temperature to stay at the right temperature for a longer time. It can be considered, in fact, a thermal booster for the forced-air cooling system. This research concerns the possibility of experimenting one possible use of PCMs in the module of a battery pack with cylindrical lithium cells, mounted on the Formula SAE Electric car.

The operating principle on which the study is to be based is the exploitation of the latent heat of liquefaction of the PCM; as the batteries heat up, the temperature of the module increases until they reach the melting point of PCM and then temperature stays stagnant until all the PCM material has been melted. Afterward, the temperature starts to increase again. In Fig. 14 the effect on a typical temperature rising ramp is represented.

The goal is therefore to delay, during the Endurance test, the achievement of the maximum temperature limit allowed for each single cell, equal to 60°C, which would force the car to stop and abandon the event. As already explained, the car of the 2022 season is equipped with a battery pack with forced air cooling. The pack consists of 6 modules and the entire package is therefore the result of the series of these 6 modules, to obtain a final 108s7p configuration. Fig. 15 shows a photo of a module.

It is therefore proposed to create a sort of “hybrid” cooling, combining PCM elements with the forced air system already present. Since the force air system acts by cooling the lateral surface of the cylindrical cells (18650), it is chosen to use metal elements (boxes) containing PCM to cool the cell tags on the busbars that connect the parallels of cells and the strings in series. The axial thermal conductivity (i.e. from positive pole to negative pole) of cylindrical lithium cells is two orders of magnitude higher than the radial one, and this can allow optimal heat transmission between PCM and cells. The initial constructive hypothesis, to be optimized, is shown in Fig. 16, involves placing the PCM in envelopes of insulating material reinforced with aluminum foil on the

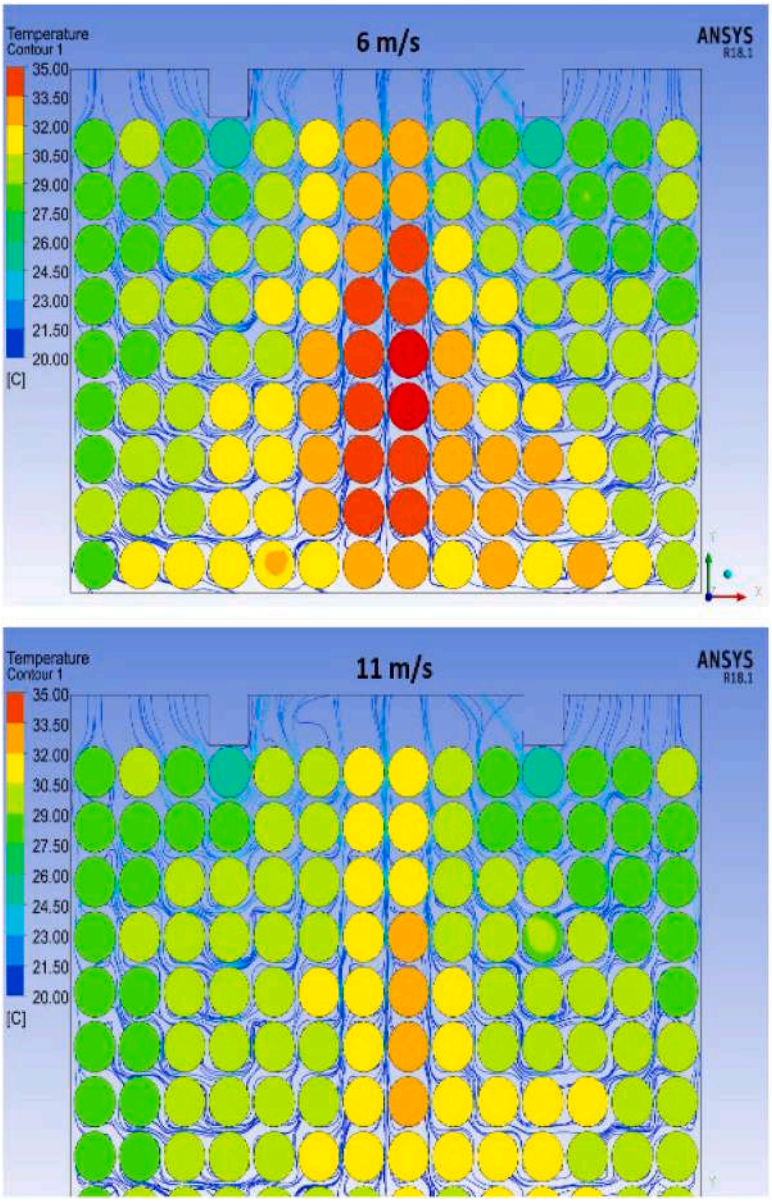

Fig. 10. Temperature distribution with air cooling at 6 m/s and 11 m/s in the 1.5 mm spacing configuration and 3 C-rate discharge, with 1.2 W/Cell of heat production.

inside, a solution that is constructively very similar to pouch battery envelopes. In this way, very thin rectangular dielectric pouches can be made which can be placed directly on the two rectangular faces of the module where the electrical connection busbars between the cells are located. In this way, in effect, the (copper) busbars, thanks to their rectangular shape, play the role of a heat sink between the cells and the PCM, with very intimate contact over a large area. The research involves a first experimental phase with one of the spare modules currently available, in order to define the main parameters of the system, and then create the boxes with PCM for the complete battery pack to be mounted on the Formula SAE car.

The simple design proposed allows on one hand to prevent PCM leakage in the liquid state and on the other hand takes advantage of the fire retardant characteristics typical of PCM [11] to increase the safety level of the entire battery pack system in case of thermal runaway of a cylindrical cell. In future works it will be very interesting to experimentally investigate the effects in a nail penetration test due to the presence of the PCM "sheets".

In this first study, no structural optimizations of the PCM will be carried out, preferring the simplicity and speed of construction, also considering the shape of the busbars particularly favorable to heat exchange, which, in fact, offer a flat plate completely available for heat exchange with the PCM. In future studies, it will be possible to evaluate the margin of improvement available with an optimized shape of the PCM panel.

An initial estimate was then made of the rough dimensioning of these thin envelopes containing PCM, on the assumption that two of them would be mounted, one on each face of the module and thus 12 in all (with 6 identical modules). A commercially available product with the following specifications was used for the PCM material (Table 5):

For the dimensioning of the system and the calculation of the PCM mass, the heat generation data of the battery pack from the acquisitions recorded during the Italy 2022 endurance race were used. The calculation model for the preliminary estimation of the system was formed on the assumption of an ideal fluid evolving in an ideal circuit, ideal cells and ideal PCM. The characteristics of the ideal fluid are zero thermal resistance and zero mechanical resistance, on the other hand, the ideal circuit has zero pressure drop, infinite circuit thermal resistance. The

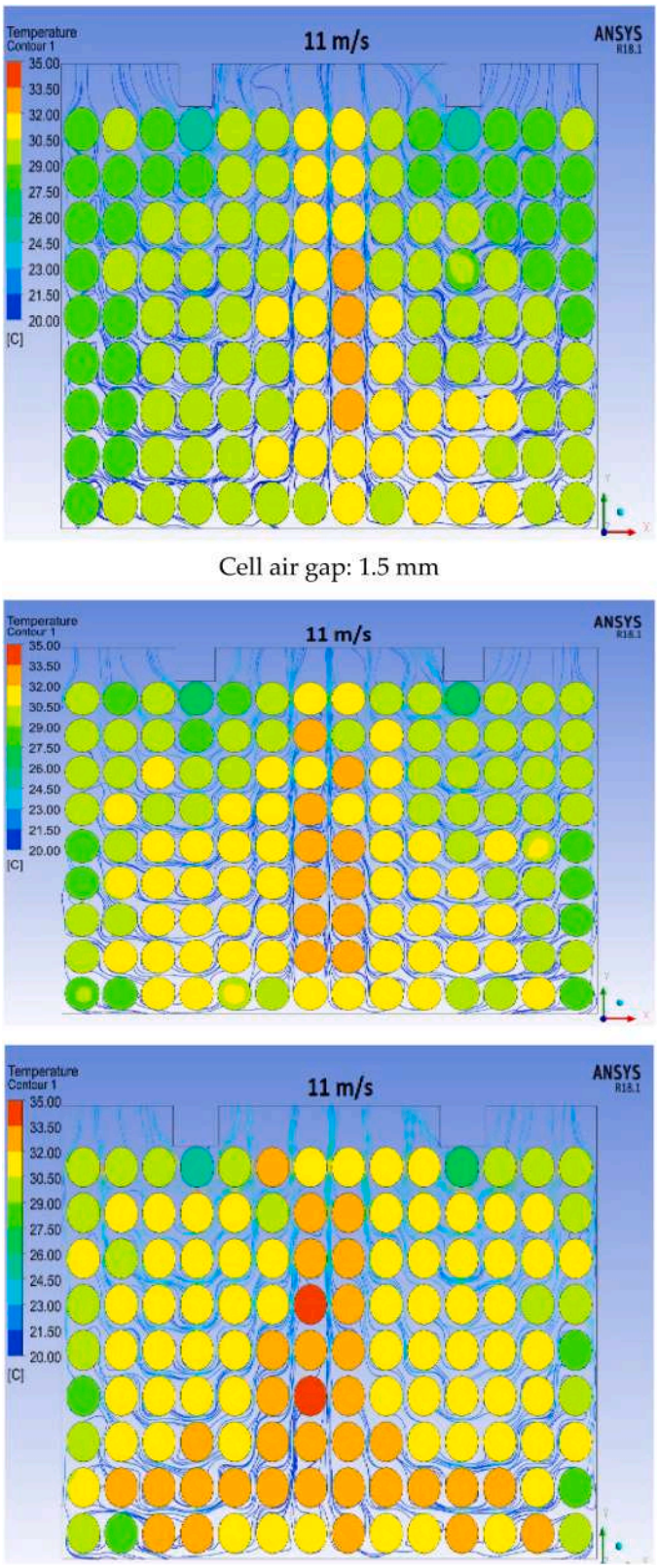

Fig. 11. Temperature distribution with air cooling at 11 m/s, 3 C-rate discharge, 1.2 W/Cell of heat production: cell air gap 1.5 mm, 2 mm and 2.5 mm

ideality lies in the fact that the cells present a constant specific heat and that the temperature distribution of the cell assembly is uniform. Finally, it was considered that the PCM melts uniformly. Then, it was determined that the PCM should assume the role of a temperature rise retarder for 200 seconds in order to keep the temperature of the cells below 50°C.

The thermal power released by the individual cell during the endurance test was 2250 J, which corresponds to a thermal power of the entire battery pack of:

$$Q_{\text{pacco2022}} = 2250 \cdot n = 1701kJ = 472Wh \tag{3a}$$

where n = 756 is the total number of cells. It was finally decided to use an amount of PCM that would allow a slowing down of the cell temperature rise by 200 seconds, so we can size, as a first approximation, the mass of PCM:

$$(P_{\text{media}} \cdot 300)/181000 = 1.16kg \tag{4}$$

where 181000 J is the value of the latent heat of liquefaction absorbed by one kg of PCM. Co-mean P was used that calculated during the first ten minutes of endurance (1.4W per cell). This results in a 20% oversizing of the PCM mass since the average thermal power generated during the entire endurance is 1.3W. The value of 1.16 kg is compatible with the design of the 2022 battery pack, since with 1.8 mm thick envelope containers, arranged on the faces of the modules in contact with the busbars, as illustrated above, the required PCM mass is obtained without changing the design of the modules and the container.

For the analysis of the thermodynamic effectiveness of the proposed solution, it was decided to experimentally test it on a single module with 4 fans as designed and two envelopes with 0.2 kg total PCM, the expected amount for each of the 6 modules of the complete package. The module was discharged with an electronic load with a current profile identical to that recorded during the Endurance 2022 test in Italy, i.e. under the same conditions already analyzed. Fig. 17 shows the comparison between the temperature of the hottest cell of the module with the PCM envelopes and without.

The thermal behavior of the cells, thanks to the simultaneous action of the forced-air cooling and the two envelope containers with the PCM with a melting point of 40°C, now appears much more satisfactory, as hoped, with a central operating zone (almost 700 s) with the temperatures remaining within the 45°C-48°C window, which is very favorable for the performance of the battery pack thanks to the low internal cell temperatures. At the end of the test, thanks to the action of the PCM, a ΔT of 10°C is achieved compared to the solution without PCM, reaching the target of staying below 50°C.

6. Conclusions

The work presented here is divided into two parts. The first phase consists of the study and optimisation of the forced-air cooling system for a battery pack for motorsport application (Formula Student). This phase made it possible to determine certain design choices that were then effectively implemented on the car for the 2022 season. In particular, the CFD simulations made it possible to determine the number, position and performance of the electric fans delegated to move the air, and as regards the geometry of the modules, made it possible to define the spacing between the cells (1.5 mm) that would make cooling more effective and homogeneous. In addition, the CFD analyses provided information on how to manage the speed of the fans in relation to the cell temperatures during the Endurance test. The choices identified in the simulation phase were then implemented on the 2022 battery pack and led to the thermal performance depicted in Fig. 13.

The second phase of the work involved a strategy for enhancing the

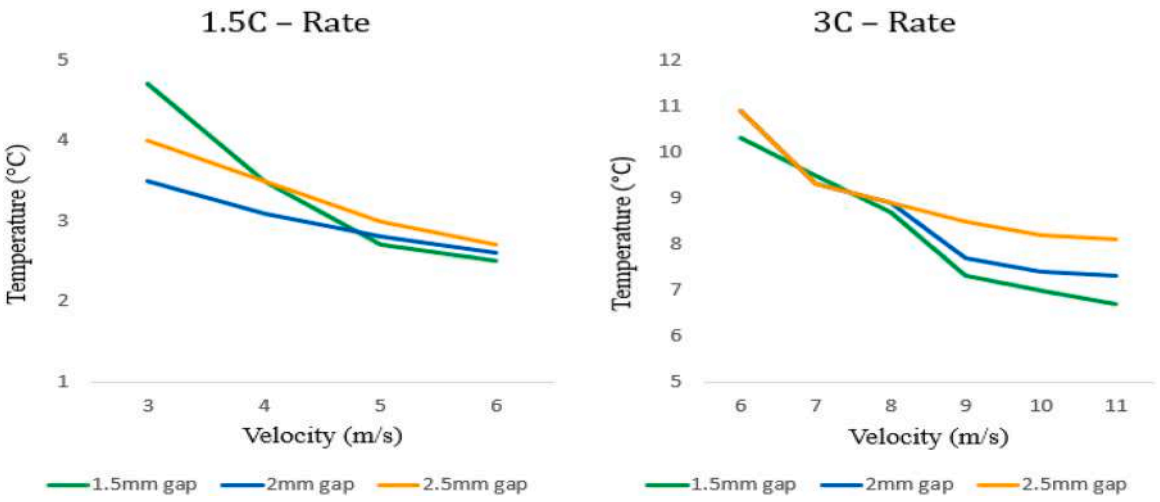

Fig. 12. ΔT distribution with different cell air gap 1.5 mm, 2 mm and 2.5 mm.

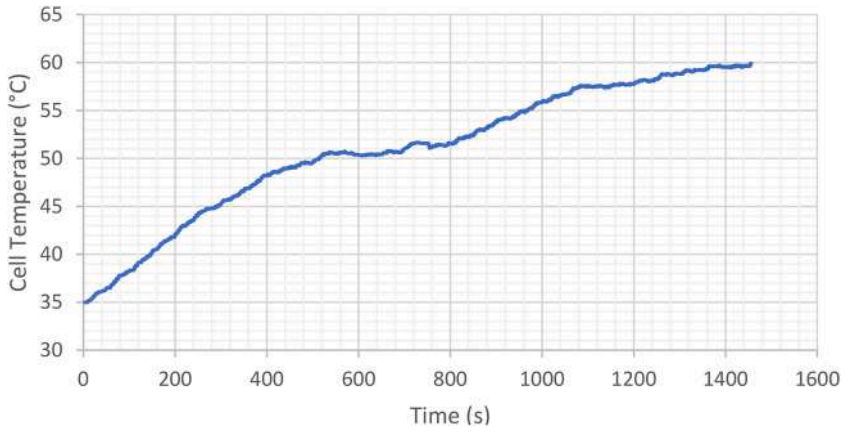

Fig. 13. Hottest **c**ell temperature during Endurance event in 2022 event.

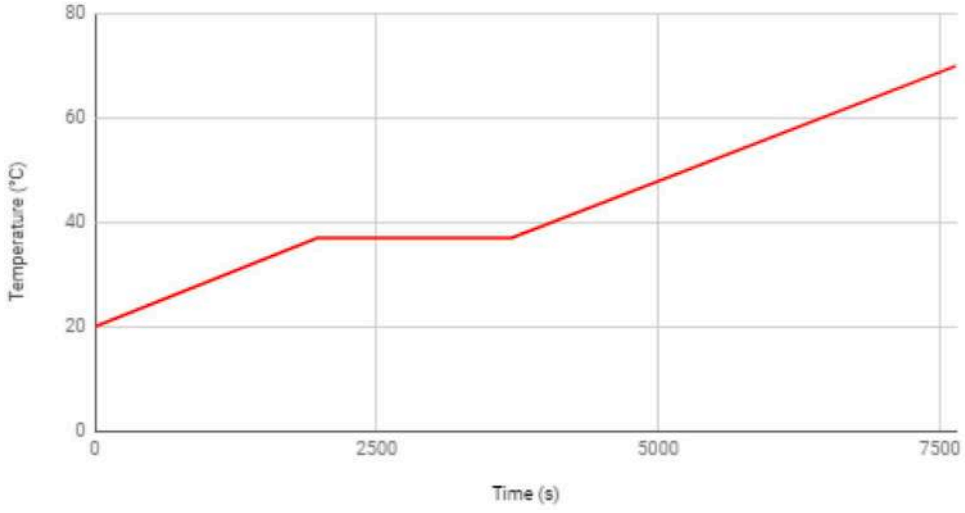

Fig. 14. Effect of the PCM melting latent heat on cells temperature.

cooling system while maintaining the design of the 2022 battery pack, by adding planar-shaped elements containing PCM material with a solid/liquid transition phase at the end of the lithium-ion cell heating phenomenon (35°C-45°C). The technological solution identified was constructively feasible and, following laboratory experimentation on a single module of the battery pack (which contains six identical ones) revealed (Fig. 17) the thermal effectiveness of the solution, which is therefore an effective, cost effective and rapid technology for an

Fig. 15. Forced air-cooled module, 2022 season car.

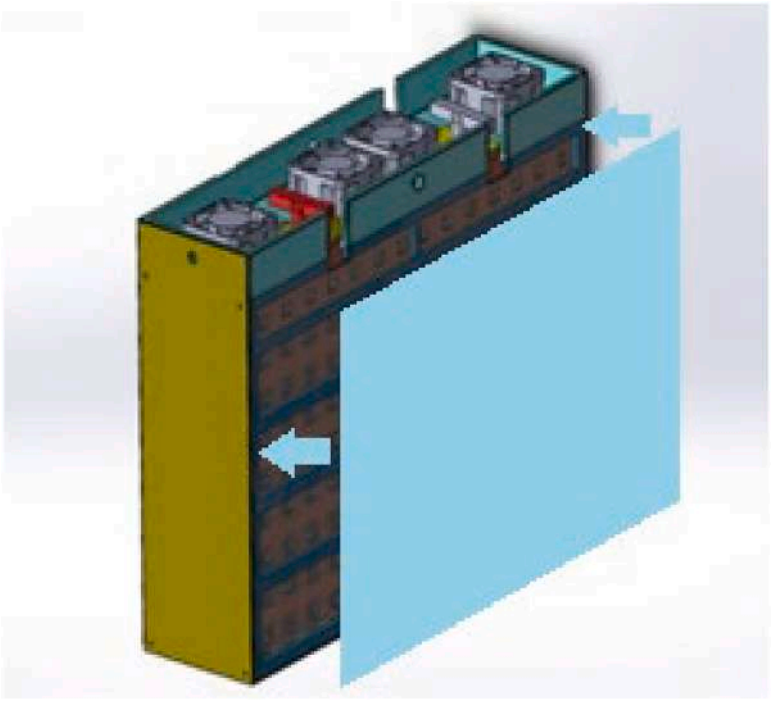

Fig. 16. PCM sheet to be applied to the front and rear faces of modules.

Table 5
Thermo-physical properties of PCM [12,13].

Parameter	Value/range
Latent heat [J kg^{-1}]	181,000
Specific heat capacity [J kg^{-1} K^{-1}]	1980
Thermal conductivity [W m^{-1} K^{-1}]	16.6
Density [kg m^{-3}]	866
Transition interval [°C]	3
Phase change temperature [°C]	40

interesting booster of the forced-air cooling system.

The results obtained clearly show the different and complementary thermal effect of the two methods of cooling the battery module and the individual cells. The forced air system has a behavior that can be defined as gradual, with an increase in the temperatures of the cells that proceeds gradually during the mission of the vehicle. This entails a "time limit" to the mission that, in the aggressive sizing of the battery pack focused on weight containment (this is a motorsport application), depends on the maximum temperature allowed by the cells and the competition regulations, equal to 60°C maximum for the hottest cell, and not on the state of charge of the pack.

In order to fully exploit the energy of the battery pack, the PCM cooling system is added, which, unlike the forced air system, intervenes only around the liquefaction threshold of the PCM, stabilizing the increase in temperature for a time that depends on its latent heat and its mass; in practice, by appropriately calibrating the mass of PCM used, the additional time interval that is introduced before reaching the threshold of 60°C for the hottest cell is determined.

The mixed forced air - PCM system therefore allows the vehicle's typical mission to be completed without problems of excessive cell temperature.

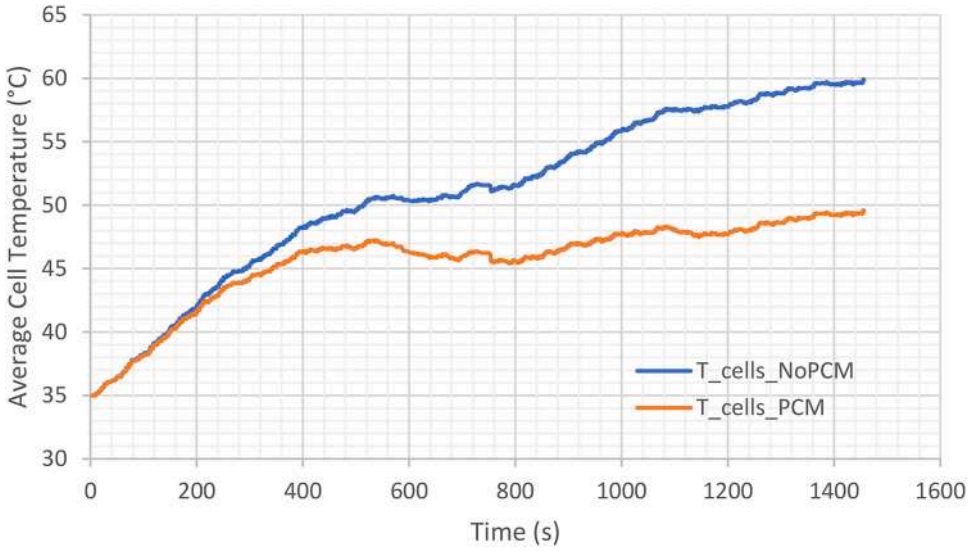

Fig. 17. PCM sheet to be applied to the front and rear faces of modules.

Funding

This research received no external funding.

Abbreviations

CFD	Computational Fluid Dynamics
PCM	Phase Change Material

CRediT authorship contribution statement

Leone Martellucci: Writing – original draft, Supervision, Funding acquisition, Data curation, Conceptualization. **Roberto Capata:** Writing – review & editing, Software, Methodology, Data curation.

Declaration of competing interest

The authors declare that they have no known competing financial interests or personal relationships that could have appeared to influence the work reported in this paper.

Data availability

Data will be made available on request.

References

[1] G. Conway, A. Joshi, F. Leach, A. García, P.K. Senecal, A review of current and future powertrain technologies and trends in 2020, Transp. Eng. 5 (2021) 100080.
[2] D.S. Cardoso, P.O. Fael, A. Espirito-Santo, A review of micro and mild hybrid systems, Energy Rep 6 (2019) 385–390.
[3] N. Nitta, F. Wu, J.T. Lee, G. Yushin, Li-ion battery materials: present and future, Mater. Today 18 (2015) 252–264.
[4] K.V.G. Raghavendra, R. Vinoth, K. Zeb, C.V.V.M. Gopi, S. Sambasivam, M. R. Kummara, I.M. Obaidat, H.J. Kim, An intuitive review of supercapacitors with recent progress and novel device applications, J. Energy Storage 31 (2020) 101652.
[5] Conte, M.; Pede, G.; Rossi, E.; Vellucci, F. Supercapacitors Research and Applications at ENEA; ENEA (Agenzia Nazionale per le Nuove Tecnologie, l'Energia e lo Sviluppo Economico Sostenibile): Kista, 2016, Sweden; pp. 2–6.
[6] A. Farmann, D.U. Sauer, Comparative study of reduced order equivalent circuit models for on-board state-of-available-power prediction of lithium-ion batteries in electric vehicles, Appl. Energy 225 (2018) 1102–1122.
[7] H. Hinz, Comparison of lithium-ion battery models for simulating storage systems in distributed power generation, Inventions 4 (2019) 41.
[8] C. Mehta, A. Sant, P. Sharma, Selection of three RC branches in equivalent circuit model of lithium-ion batteries for improved accuracy, Turk. J. Comput. Math. Educ. 12 (2021) 1478–1489.
[9] A. Morandi, A. Lampasi, A. Cocchi, F. Gherdovich, U. Melaccio, P.L. Ribani, C. Rossi, F. Soavi, Characterization and model parameters of large commercial supercapacitor cells, IEEE Access 9 (2021) 20376–20390.
[10] V.H. Johnson, Battery performance models in ADVISOR, J. Power Sources 110 (2002) 321–329.
[11] c Jingwen Weng, Qiqiu Huang, Xinxi Li, Guoqing Zhang, Dongxu Ouyang, Mingyi Chen, Anthony Chun Yin Yuen, Ao Li, Eric Wai Ming Lee, Wensheng Yang, Jian Wang, Xiaoqing Yang, Safety issue on PCM-based battery thermal management: material thermal stability and system hazard mitigation, Energy Storage Materials 53 (2022) 580–612. Elsevier.
[12] Available online: https://www.spscap.com/Data-Sheet/Data-Sheet_SCP-STA-Series_2017-2_EN-.pdf (accessed on June 2017).
[13] R. Sabbah, R. Kizilel, J.R. Selman, S. Al-Hallaj, Active (air-cooled) vs. passive (phase change material) thermal management of high power lithium-ion packs: limitation of temperature rise and uniformity of temperature distribution, J. Power Sources 182 (2008) 630–638.